Eur. Phys. J. D **4**, 1–6 (1998)

THE EUROPEAN PHYSICAL JOURNAL D

Electron multiplicity in slow collisions of Ar^{8+} ions with C_{60}

S. Martin, J. Bernard, L. Chen, A. Denis, and J. Désesquelles

Laboratoire de Spectrométrie Ionique et Moléculaire[a], Université Claude Bernard, Lyon I, Bâtiment 207, Campus de la Doua, 69622 Villeurbanne Cedex, France

Received: 25 March 1998 / Received in final form and Accepted: 9 June 1998

Abstract. Electron capture by Ar^{8+} in collisions with C_{60} fullerene has been investigated using coincident measurements of the number n of ejected electrons, the mass and charge of multicharged C_{60}^{r+} recoil ions and their fragments C_m^{i+} and the final charge state of outgoing projectiles $Ar^{(8-s)+}$ ($1 \leq s \leq 7$). The number of captured electrons r is the sum of the numbers of stabilized and emitted electrons: $r = n + s$. The ratio n/s decreases by a factor three with s increasing from 1 to 7 showing that the multiply excited states populated by capture of a large number of electrons are rather stable against auto-ionisation. Each kinetic energy spectrum of Ar^+ and Ar^{2+} projectiles is composed of two peaks which we attribute to collisions "inside" and "outside" the C_{60} cage. The measured energy shift of the projectile $\Delta E = 0.3$ keV is consistent with the corresponding energy loss $\Delta E_c = 0.4$ keV in a carbon foil with an equivalent thickness. Inside collisions are characterized by a strong dissociation of recoil ions into light monocharged fragments and by a high multiplicity of ejected electrons.

PACS. 36.40.Qv Stability and fragmentation of clusters – 34.70.+e Charge transfer

1 Introduction

Since fullerenes became available in substantial quantities, collisions of fast and slow highly charged ions with C_{60} have received much attention [1–12]. At low impact energy the dominating processes are single – and multiple – electron captures which have been previously studied in collision of multiply charged ions with multielectron atomic targets. C_{60} can actually be considered as an atomic target with a great number of nearly equivalent electrons (60 π electrons) for large impact parameter collisions in which electron capture occurs at a distance much larger than the radius (6.7 a.u.) of the C_{60} cage. When the impact parameter is slightly larger than the C_{60} radius, some kind of surface interaction can be considered. As it is observed with a real surface, the projectile can capture a great number of electrons and its final charge state could be very low. However, it is noteworthy that the interaction time is much shorter in collisions with C_{60} than in grazing incidence collisions with a surface. In the case of head-on collisions in which the impact parameter is smaller than the C_{60} radius, a comparison can be made with beam-foil interaction of ions passing through a thin carbon foil, particularly in connection with final projectile charge state distributions and energy loss.

Several experiments have been performed on $Ar^{8+}-C_{60}$ collisions at low energy ($v < 1$ a.u.) during last few years [1,2,10] establishing interesting results. At large impact parameter ($R \simeq 20$–25 a.u.), the excitation energy of C_{60} is relatively low, leading to observation of multicharged fullerene ions C_{60}^{r+} ($1 \leq r \leq 6$) [1]. At smaller impact parameter, the C_{60} excitation energy becomes significant and fragmentation processes take place. Walch *et al.* [1] reported C_{60} fragmentation spectra and absolute cross-sections for stabilization of $s = 1$ to 8 electrons on the argon projectile. A somewhat unexpected result was a slight increase of cross-section for $s = 6$ and 7, coming after a continuous decrease with s increasing from 1 to 5. This "hump" was associated with "inside" collisions and destruction of C_{60}. Experimental barrier radii deduced from measured cross-sections for transfer of 1 to 6 electrons were found to be in good agreement with those obtained from a classical over the barrier model (CBM) corrected for polarization effects [1]. From the total cross-section, summed over all final charge states of the argon projectiles (4.4×10^{-14} cm^2), and confirmed by a measurement of Selberg *et al.* [2] (4.6×10^{-14} cm^2), they deduced the firstbarrier radius (22–24 a.u.) comparable to the CBM values, while the destruction cross-section (1.5×10^{-14} cm^2) was found to be larger than the geometrical C_{60} cross-section (0.4×10^{-14} cm^2). Besides the total reaction cross-section, Selberg *et al.* [2] presented energy gain distributions for $s = 1$ and 2 in a non-coincident experiment. They discussed the results within a qualitative model in which the transient localization of the positive charge on the surface of C_{60} was taken into account. Thumm *et al.* [4] have developed theoretical models for the electronic structure of C_{60} in order to predict the capture levels, ejected electron numbers and evolution

[a] UMR-CNRS 5579

of projectile and target charge states. In these models, most of the Auger relaxation channels are sufficiently slow to be neglected during the collision time which here is less than 6 fs and the cage transit time of about 1 fs.

In these early measurements, the initial number of electrons captured by the projectile before auto-ionisation, *i.e.* the number of active electrons in a capture process, is not known. Contrary to the case of an atomic target, this number can not be directly obtained by measuring the charge state of the recoil ion. One could imagine to determine it by collecting all charged fragments, but it is not easy to do. It can be done in another way by adding the number of electrons stabilized on the argon projectile to the number n of free electrons $r = s+n$. We present in this paper such an experiment in which the number of emitted electrons (n) and the number of stabilized electrons (s) were measured for each final charge state ($8-s$) of the projectile for $Ar^{8+} + C_{60}$ collisions at 56 keV energy. The number of emitted electrons has been measured up to 11, a number which is exceeding the initial charge state of the incoming projectile Ar^{8+}. An explanation based on the populations of multiply excited states in the argon projectile will be proposed to account for the variation from 1.2 to 0.3 of the ratio n/s of the number of ejected electrons to the number of stabilized electrons when s increases from 1 to 7. Contributions from soft and head on collisions will be detailed.

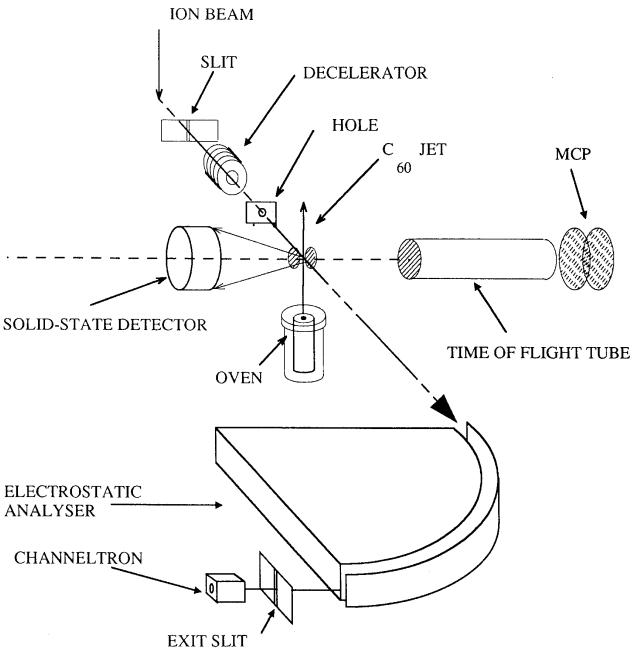

Fig. 1. Schematic diagram of the experimental arrangement. Note that the intermediate electrode inserted between the electron detector and the collision cell has not been drawn.

2 Experiment

The Ar^{8+} beam for the present experiment was provided by the electron cyclotron resonance ion source Nanogan equipped with a 4 W, 10 GHz microwave generator installed on the Danfysik accelerator at Lyon University. Up to 2 μA Ar^{8+} ion current could be extracted from the source at 20 kV but, in the coincidence experiment, we used 56 keV Ar^{8+} beam ($v \simeq 0.24$ a.u.) of only a few 10 pA collimated to about 500 micrometers in diameter. The ion beam crossed a thermal fullerene molecular beam produced by evaporating sample powder containing about 99.9% C_{60} and 0.1% C_{70} in an oven (540 °C) ended by a 1 mm aperture . Recoil ions and electrons produced in the collision region were extracted at right angles to the beams by an electric field of 1 kV/cm over 5 mm (Fig. 1). The deflection of the projectile ion beams induced by the field was compensated by two steerers located upstream and downstream from the extraction plates. The outgoing projectiles were charge state analyzed by a 90° cylindrical analyzer ($R = 150$ mm) and a channel electron multiplier. The extracted recoil ion's charge states and masses were determined by the time of flight technique. A 1 kV/mm field was applied over 3 mm to accelerate ions towards a 150 mm long field free drift tube and a channel plate multiplier assembly with the front plate biased at -4.5 kV. The extracted electrons were accelerated through an intermediate electrode biased at 2.5 kV towards a semi conductor detector (Canberra, Passivated Implanted Planar Silicon PIPS 150-12-300) biased at 27 kV. The pulse height of the electron detector signal is proportional to the number of electrons collected by the PIPS detector for each collisionnal event. Further details on the electron detection can be found elsewhere [11]. In a test experiment the collection and detection efficiencies have been found to be 98% for electrons and about 50% for monocharged ions. A Time to Digital Converter (TDC 3377, Le Croy) was used in the common stop mode. The projectile signal, 8 μs delayed, was used as the reference common stop hit and the recoil ion fragment's signals were sent to a multi-hit channel. The pulse of the electron signal was suitably delayed and sent to an Analog to Digital Converter (ADC 811, Ortec) triggered by the projectile signal.

3 Results

The pulse height of the electron PIPS signals and the time of flight of the recoil ions have been measured in coincidence with outgoing $Ar^{(8-s)+}$ projectiles successively recorded from Ar^{7+} to Ar^{+} which have stabilized $s = 1$ to 7 electrons. Two types of two-dimensional spectra have been registered. The first ones are called multistop spectra which record all hits due to recoil ions and ionized fragments occurring in an event. The second ones are called monostop spectra in which we only stored the hit due to the heaviest, last-detected, fragment. Most differences between the two types of 2D spectra are expected for $s > 2$ when C_{60}^{r+} ions are essentially fragmented into monocharged C_n^+ ions. In this cases, the C_n^+ distribution is better reproduced by the multistop spectra while the number of collisionnal events is obtained using monostop detection. Examples of monostop scatter plots are shown

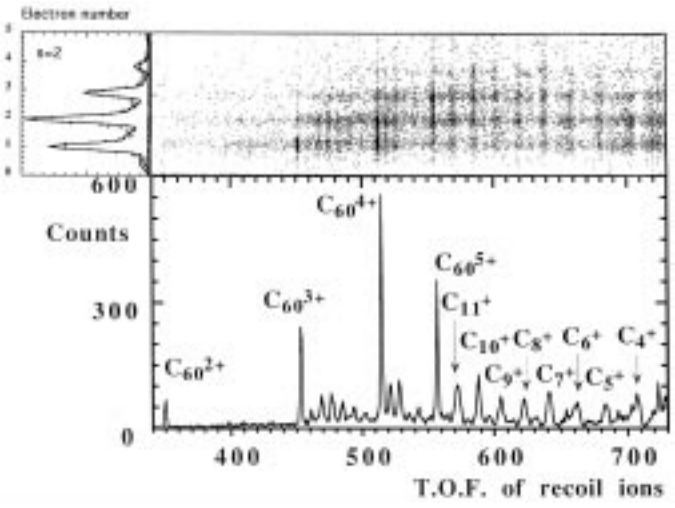

Fig. 2. A typical two dimensional spectrum and its projections. The electron multiplicity was measured in concidence with the time of flight of recoil ions and ionized fragments for the projectile final charge state 6+ after $Ar^{8+}-C_{60}$ collisions ($s = 2$). Fragments were due to evaporation and fission of C_{60}^{3+}, C_{60}^{4+}, and C_{60}^{5+} primary ions.

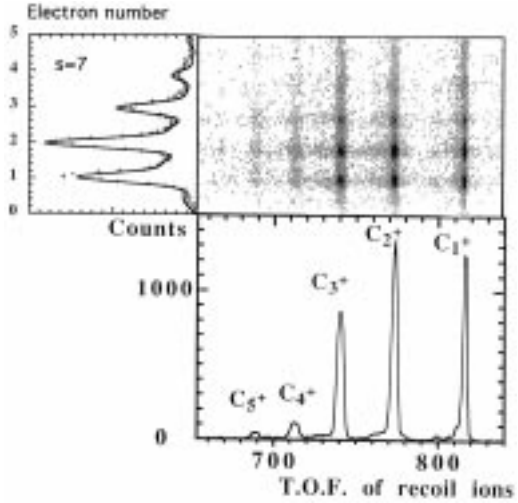

Fig. 3. Same coincidence spectrum as in Fig. 2 but for monocharged outgoing projectiles ($s = 7$). Initially populated C_{60}^{8+}, C_{60}^{9+} and C_{60}^{10+} ions explode in small fragment ions, essentially $C^{+}-C_3^{+}$.

in Figure 2 for outgoing Ar^{6+} ($s = 2$) and in Figure 3 for outgoing Ar^{+} ($s = 7$).

The projections of the 2D spectra onto the vertical and horizontal axis give the electron number distributions and the recoil ion spectra respectively. In Figure 2, the main features of the ion charge state projection are the strong C_{60}^{3+}, C_{60}^{4+} and C_{60}^{5+} peaks which have to be associated with the $n = 1$, 2 and 3 electron peaks of the electron multiplicity projection ($r = n+2$). The C_{60-2m}^{3+} and C_{60-2m}^{4+} peaks issued from primary C_{60}^{3+}, C_{60}^{4+} and C_{60}^{5+} recoil ions have to be associated to 1, 2 or 3 electrons depending on the break-up mechanisms, evaporation of neutrals C_2 or fission of C_2^{+} or C_4^{+} ions [11]. The C_n^{+} fragments, issued from highly charged parent fullerene, mainly C_{60}^{5+}, contribute to the three electron peak. Ghost spots as (C_{60}^{4+}, $1e$) and (C_{60}^{5+}, $2e$) are present in the 2D spectrum. We have verified that they are entirely due to backscattering of electrons in the PIPS detector [13]. They have been taken into account to determine the true electron distributions. The initial C_{60}^{r+} populations are given by the corrected electron statistics while the intensities of the C_{60}^{3+}, C_{60}^{4+} and C_{60}^{5+} peaks give the number of primary recoil ions stable against evaporation, fission and multifragmentation. Here we measured as stable any C_{60} ion with a lifetime longer than its flying time from the collision region to the drift tube ($\simeq 400$ ns). The 2D spectrum is very different for collisions with high neutralization of the argon ion beam (Fig. 3). Fullerene ions are absent from the time of flight spectrum whereas the mean features relate to light monocharged ions, principally C_4^{+}, C_3^{+}, C_2^{+} and C^{+} , which result from the multifragmentation of C_{60}^{8+}, C_{60}^{9+}, C_{60}^{10+} and C_{60}^{11+} ($r = n + s$ with $s = 7$ and $1 \leq n \leq 4$). However, the emitted electron statistics for $s = 7$ resembles that obtained for $s = 2$, so that the further electrons captured from C_{60} are essentially used to neutralize the projectile as soon as $s > 2$.

2D spectra have been recorded for $s = 1$ to 7. They have been corrected for recoil ion detection efficiencies. The probability for detecting at least one fragment in a collisionnal event depends on the number of fragments, their mass and their charge. It was 100% for $s = 5$, 6 and 7 when fullerenes break up into many very light monocharged fragments. It was found equal to 0.93 and 0.87 for $s = 4$ and $s = 3$ when fullerenes break up into several light fragments. When recoil ions are essentially heavy fullerene ions, it was found equal to 0.75 for $s = 2$ and 0.4 for $s = 1$. The detail of the procedure to determine the efficiencies will be presented in a forthcoming paper. Relative cross-sections σ_r^s to capture r electrons and to stabilize s of them have been deduced from the corrected measured electron spectra. They have been calibrated by using the total cross-section $\sigma_t = 4.4 \times 10^{-14}$ cm^2 of Walch *et al.* [1] to give the absolute cross-sections of Figure 4. Result can not be directly compared to global measurements of Walch *et al.* which gave the cross-section for electron capture *versus* the number of electrons kept (stabilized) by the projectile whatever the number (r) of active electrons may be. However, there is a general good agreement between their cross-sections and our cross-sections summed over the number of active electrons. Particularly, the hump they found for $s = 5$–8 clearly appears on Figure 4 but our cross-sections $\sum \sigma_r^6$ and $\sum \sigma_r^7$ are slightly different of their values. By summing our partial cross-sections over s, we obtain the capture cross-section *versus* the number of active electrons r up to $r = 11$. In Figure 5, results are compared to calculated cross-sections obtained using the classical barrier model without screening and the theoretical ionisation potential values $I_r(\text{eV}) = 7.7 + 3(r-1)$ from [14]. For $r = 1-5$, there is a good agreement. However, for high r values, theoretical cross-sections are overestimated. The model has then to be modified by including screening for the electrons captured in low levels, which

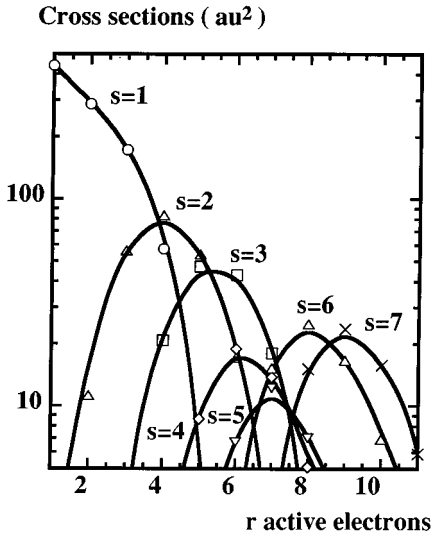

Fig. 4. Cross sections *versus* number of active electrons ($r = n + s$) in $Ar^{8+}-C_{60}$ collisions for $s = 1$–7 stabilized electrons. The total cross-section measured by Walch *et al.* [1] has been used for calibrating the ensemble of curves. The cross-section increase for $s = 6$ and 7 is partially due to head – on collisions.

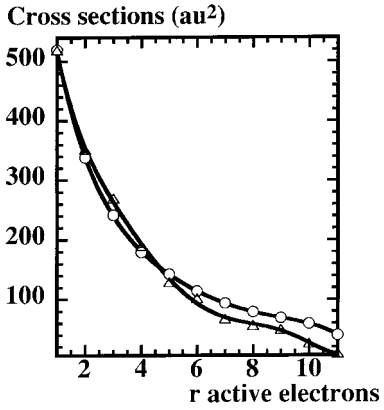

Fig. 5. Electron capture cross-sections summed over s *versus* number of active electrons r (Δ). Comparison with theoretical values resulting from the classical overbarrier model ($\circ$).

gives lower cross-sections in better agreement with experimental data. Errors in ionisation potentials could contribute to the observed discrepancies too [4,15].

To learn more about the stability of the argon multi-excited ions, the number of emitted electrons n has been compared to the number s of electrons and the number r of active electrons in a collisionnal event. For that, the average number of ejected electrons $\langle n \rangle$ and the ratio $\langle n \rangle / s$ were plotted as a function of s (Fig. 6). This ratio decreases from 1.2 to 0.3 with s increasing from 1 to 7. When four electrons are captured ($r = 4$), two of them ($s = 2,\ \langle n \rangle = 2$) are on average stabilized on the projectile whereas among seven electrons captured ($r = 7$) only two are ejected and five are stabilized ($\langle n \rangle = 2,\ s = 5$). As soon as two electrons are auto-ionized the further ones are generally captured on non-auto-ionizing levels of the projectile. These somewhat unexpected results can be compared with predictions of the population dynamics of projectile levels by Thumm *et al.* [4] for soft collisions of C_{60} with 80 keV Ar^{8+} ions. Following their calculations, the first electrons are captured on shells $n = 7$ and 6 and for example, for an impact parameter $b = 15$ a.u., an ingoing Ar^{8+} ion can capture five electrons in a (7, 6, 6, 5, 5) multi excited state which finally, after fast and slow Auger electron emission, gives a stable outgoing Ar^{6+} ($s = 2$). This kind of event corresponds to the spot associating C_{60}^{5+} with the electron multiplicity $n = 3$ in the 2D spectrum of Figure 2. However, in Thumm's calculations, the number of Auger electrons is at most one. Furthermore, when the number of electrons captured in the shells 4–6 increases, the formed multiexcited states could be expected to decay by emission of a large number of electrons which, experimentally, is not the case. It seems that a small number of Auger transitions is sufficient to populate outgoing argon ions in too low-lying shells to be significantly autoionizing.

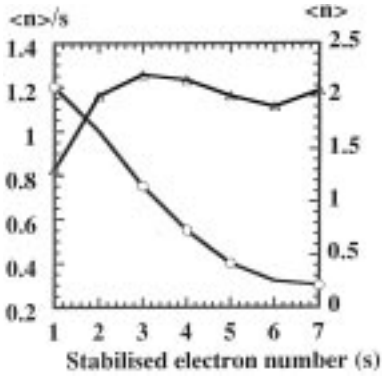

Fig. 6. Stabilized and ejected electrons. Empty circles: average ejected electron number (n) divided by number of electrons stabilized on the projectile (s) as a function of s. Empty triangles: $\langle n \rangle$ as a function of s.

A more detailed look at the charge transfer and fragmentation processes has been obtained by recording recoil ions in coincidence with outgoing projectiles. By scanning the electric field voltage applied to the cylindrical analyzer step by step, two-dimensional spectra were obtained in which each point of the spots corresponds to a given fragment associated with an argon ion having stabilized a given number of electrons and having undergone a given energy change. Figure 7 shows a typical 2D monostop spectrum obtained for $s = 5$, 6 and 7 where mean features are $C^+-C_4^+$ fragments. The vertical projection shows that the energy change is not uniformly distributed for $s = 6$ and $s = 7$. Both peaks appear as the sum of a strong high energy component that we call the peak *OUT* and a small broad lower energy component, called *IN*. The peak *IN* is attributed to central or, more precisely, inside collisions and the peak *OUT* to peripheral ones. The kinetic energy losses of 300 ± 50 eV and 350 ± 50 eV, measured for the peaks *IN* corresponding to $s = 7$ and 6 respectively, are consistent with the energy loss of 56 keV Ar^{8+} ions in a thin carbon foil which amounts to about 80 eV per Å [16]. A loss of 350 eV corresponds to an effective

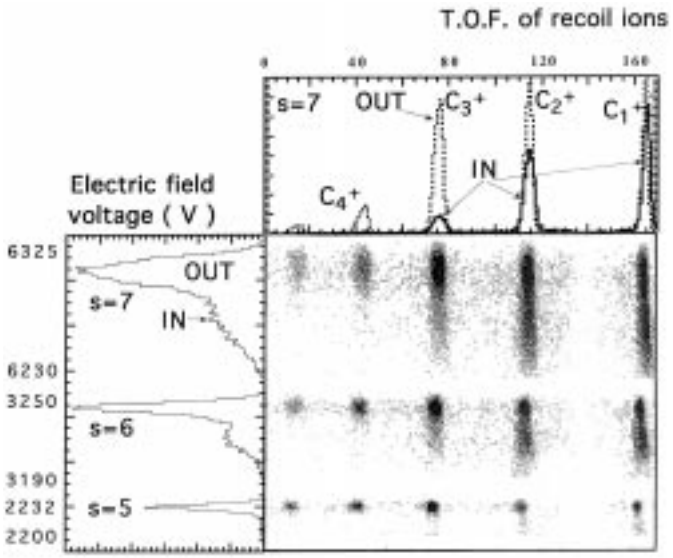

Fig. 7. Two-dimensional spectrum and its projections. Time of flight of recoil fragments was measured in coincidence with projectile kinetic energy for $s = 5$, 6 and 7. Peaks *IN* and *OUT* are associated with collisions of Ar^{8+} ions inside and outside C_{60} cages. In recoil ion spectra for $s = 7$, lighter fragments were observed for inside collisions in which excitation energy is higher.

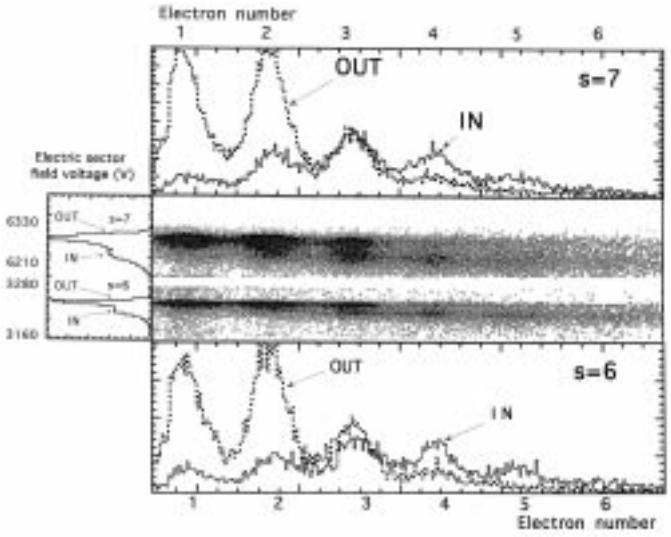

Fig. 8. Two-dimensional spectra and their projections. Electron multiplicity was measured in coincidence with projectile kinetic energy for $s = 6$ and 7. The average number of electrons ejected in inside collisions exceeds by about two units that of peripheral collisions.

target thickness of 4.5 Å which is comparable to the average thickness 3 Å of the C_{60} shell. The total inside collision cross-section, obtained by summing the measured 0.2, 1.2 and 1.1×10^{-14} cm^2 *IN* component cross-sections associated to $s = 5$, 6 and 7, amounts to 3.5×10^{-14} cm^2. It is in good agreement with the 4.2×10^{-14} cm^2 geometrical cross-section of a 7.4 Å diameter C_{60} cage. Moreover, the projectile final charge states are lower after central collisions than after peripheral collisions and tend to that expected for a beam-foil interaction [17,18]. The differential horizontal projection of the 2D spectrum (Fig. 7) according to the projectile *IN* and *OUT* components indicates that C_3^+, C_4^+ fragments are for the most part related to the *OUT* component and C^+ and C_2^+ fragments are due to both of them. So comparing to peripheral collisions (*OUT*), central collisions (*IN*) give smaller fragments, showing that high excitation energy leads to high vaporization of C_{60}. Further differences have been established between peripheral and central collisions using 2D coincidence spectra of projectiles and emitted electrons (Fig. 8). The electron multiplicities are very different. On an average, two more electrons were detected for central collisions which can tentatively be attributed to electron emission from C_{60}.

In summary, by using coincidence measurements between outgoing projectiles in their final charge state, recoil ions and ejected electrons, we were able to show great differences between central and peripheral collisions. The peripheral collisions can lead to the production of final charge states of Ar^{q+} down to $q = 1$ just as the central ones but in a smaller proportion. The ratio between ejected and stabilized electrons decreases with s increasing from 1 to 7 in such a way that, for $s > 2$, almost all further electrons captured from C_{60} are stabilized on the projectile. It shows that the multiexcited states populated in these collisions become more stable against Auger process when the number of electrons increases. Central collisions are characterized by a large energy loss of the projectile, contrary to the cases of C_{60} peripheral collisions and of collisions between highly charged ions and atoms in which there is always a kinetic energy gain. They also lead to a complete vaporization of C_{60} and to an increase in the number of ejected electrons.

This work was supported in part by the Region Rhône-Alpes under grant n° 97027-223 and -283, Convention Recherche, Programme Emergence.

References

1. B. Walch, C.L. Cocke, R. Voelpel, E. Salzborn, Phys. Rev. Lett. **72**, 1439 (1994).
2. N. Selberg, A. Bárány, C. Biedermann, C.J. Setterlind, H. Cederquist, A. Langereis, M.O. Larsson, A. Wännström, P. Hvelplund, Phys. Rev. A **53**, 874 (1996).
3. A. Bárány, C.J. Setterlind, Nucl. Instrum. Meth. Phys. Res. Sect. B **98**, 184 (1995).
4. U. Thumm, T. Bastug, B. Fricke, Phys. Rev. A **52**, 2955 (1995); U. Thumm, Phys. Rev. A **55**, 479 (1997).
5. T. Lebrun, H.G. Berry, S. Cheng, R.W. Dunford, H. Esbensen, D.S. Gemmel, E.P. Kanter, W. Bauer, Phys. Rev. Lett. **72**, 3965 (1994).
6. J. Jin, H. Khemliche, M.H. Prior, Z. Xie, Phys. Rev. A **53**, 615 (1996).
7. H. Shen, P. Hvelplund, D. Mathur, A. Bárány, H. Cederquist, N. Selberg, D.C. Lorents, Phys. Rev. A **52**, 3847 (1995).

8. Y. Nakai, A. Itoh, T. Kambara, Y. Bitoh, Y. Awaya, J. Phys. B **30**, 3049 (1997).
9. H. Cederquist (private communication).
10. J. Bernard, L. Chen, A. Denis, J. Désesquelles, S. Martin, Phys. Scripta T **73**, 286 (1997).
11. S. Martin, L. Chen, A. Denis, J. Désesquelles, Phys. Rev. A **57**, (1998).
12. T. Schlathölder, R. Hoekstra, R. Morgenstern, J. Phys. B **31**, 1321 (1998).
13. F. Aumayr, G. Lakits, H. Winter, Appl. Surf. Sci. **47**, 139 (1991).
14. C. Yannouleas, U. Landman, Chem. Phys. Lett. **217**, 175 (1994).
15. H. Steger, J. Holzapfel, A. Hielscher, W. Kamke, I.V. Hertel, Chem. Phys. Lett. **234**, 455 (1995).
16. T. Schenkel, A.V. Hamza, A.V. Barnes, D.H. Schneider, Phys. Rev. A **56**, 1701 (1997); T. Schenkel *et al.*, Phys. Rev. Lett. **79**, 2030 (1997).
17. J.F. Ziegler, J.P. Biersack, U. Littmark, *The Stopping and Range of Ions in Solids*, Vol. 1 (Pergamon, New York, 1985).
18. R.O. Sayer, Rev. Phys. Appl. **12**, 1543 (1977).